

Heterogeneity of Specific Gas Volume Changes

A New Tool to Plan Lung Volume Reduction in COPD

Caterina Salito, PhD; Livia Barazzetti, MSc; Jason C. Woods, PhD; and Andrea Aliverti, PhD

OBJECTIVE: The aim of this work was to investigate if regional differences of specific gas volume (SVg) in the different regions (lobes and bronchopulmonary segments) in healthy volunteers and patients with severe emphysema can be used as a tool for planning lung volume reduction (LVR) in emphysema.

METHODS: CT scans of 10 healthy subjects and 10 subjects with severe COPD were obtained at end-inspiration (total lung capacity [TLC]) and end-expiration (residual volume [RV]). For each subject, ΔSVg ($\Delta SVg = SVg_{TLC} - SVg_{RV}$, where SVg_{TLC} and SVg_{RV} are specific gas volume at TLC and RV, respectively) vs ΔV ($\Delta V = V_{TLC} - V_{RV}$, where V_{TLC} and V_{RV} are lung volume at TLC and RV, respectively) was plotted for the entire lung, each lobe, and all bronchopulmonary segments. For each subject, a heterogeneity index (HI) was defined to quantify the range of variability of $\Delta SVg/\Delta V$ in all bronchopulmonary regions.

RESULTS: In patients with COPD, SVg_{TLC} and SVg_{RV} were significantly higher and ΔSVg variations lower than in healthy subjects ($P < .001$). In COPD, $\Delta SVg/\Delta V$ slopes were lower in upper lobes than in lower lobes. In healthy subjects, the entire lung, lobes, and bronchopulmonary segments all showed similar $\Delta SVg/\Delta V$ slopes, whereas in COPD a high variance was found. As a consequence, HI was significantly higher in subjects with COPD than in healthy subjects (0.80 ± 0.34 vs 0.15 ± 0.10 , respectively; $P < .001$).

CONCLUSIONS: SVg variations within the lung are highly homogeneous in healthy subjects. Regions with low $\Delta SVg/\Delta V$ (ie, more pronounced gas trapping) should be considered as target areas for LVR. Regions with negative values of $\Delta SVg/\Delta V$ identify where collateral ventilation is present. HI is helpful to assess the patient in the different stages of disease and the effect of different LVR treatments.

CHEST 2014; 146(6):1554-1565

Manuscript received December 4, 2013; revision accepted May 26, 2014; originally published Online First June 19, 2014.

ABBREVIATIONS: HI = heterogeneity index; HU = Hounsfield unit; LAA = low attenuation area; LAA-856 = lung pixels with an attenuation of ≤ -856 HU on expiratory CT scan; LAA-950 = lung pixels with an attenuation of ≤ -950 HU on inspiratory CT scan; LLL = left lower lobe; LUL = left upper lobe; LVRS = lung volume reduction surgery; ROI = region of interest; RLL = right lower lobe; RUL = right upper lobe; RV = residual volume; SVg = specific gas volume; SVg,r = regional specific gas volume; TLC = total lung capacity

AFFILIATIONS: From the TBMLab (Drs Salito and Aliverti and Ms Barazzetti), Dipartimento di Elettronica, Informazione e Bioingegneria, Politecnico di Milano, Milan, Italy; the Center for Pulmonary Imaging

Research (Dr Woods), Cincinnati Children's Hospital Medical Center, Cincinnati, OH; and the Department of Physics (Dr Woods), Washington University, St. Louis, MO.

FUNDING/SUPPORT: This work was supported by the National Institutes of Health [Grant R01-HL090806].

CORRESPONDENCE TO: Caterina Salito, PhD, Dipartimento di Elettronica, Informazione e Bioingegneria, Politecnico di Milano, P.zza L. da Vinci, 32, 20133 Milano, Italy; e-mail: caterina.salito@polimi.it

© 2014 AMERICAN COLLEGE OF CHEST PHYSICIANS. Reproduction of this article is prohibited without written permission from the American College of Chest Physicians. See online for more details.

DOI: 10.1378/chest.13-2855

In the past years there have been intense research efforts to develop precise imaging biomarkers relevant to COPD and other lung diseases. Analysis of lung ventilation is explored via MRI with hyperpolarized gases, such as ^3He ¹⁻³ or ^{129}Xe .⁴ CT imaging allows densitometric measurements of the lung, and its ability to quantify trapped gas has been shown.⁵⁻⁸

Research into new biomarkers has been mirrored by efforts at trapped-gas reduction via new invasive and minimally invasive interventions, such as stent-supported airway bypass⁹ and endobronchially installed, one-way exit valves.¹⁰ Endobronchial treatments are still in investigational phases; preliminary results are varied and may suffer from the lack of a precise imaging biomarker. Recently, it has been shown that quantitative CT scan target volume¹¹ and regional perfusion¹² analysis may help to identify lobar exclusion and to select the most responsive patients to endobronchial valve treatment. Measurements of changes in specific gas volume (SVg) via CT scan may not only be an excellent biomarker but may also provide specific regional information that can aid in surgical planning and evaluation posttreatment. SVg is defined as volume of gas per gram of tissue (mL/g) and is derived pixel-by-pixel from CT images of lung density.^{6,8} It can be extracted from CT images by converting the Hounsfield unit (HU) value to a measure of specific volume, which is a more physiologically meaningful measure. This

method has been introduced by Coxson et al^{5,6} in studies assessing regional lung volumes and by Salito et al⁸ in studies on an animal model of airway obstruction and on emphysematous lungs *in vivo*.⁷ SVg is necessarily quantitative, and it can be used regionally¹³ and globally.

The aim of this work was to evaluate if heterogeneity of SVg and its changes with lung volume can be considered a useful tool for planning lung volume reduction surgery (LVRS) in patients with severe emphysema who are candidates for LVRS. We hypothesized that in the different regions of normal lungs, variations of SVg with lung volume are very similar throughout the lung. Conversely, in emphysema there are regions where gas is trapped, and regional SVg should vary little with volume, in contrast to other regions where regional SVg variations are greater than normal and the heterogeneity of variations of SVg with lung volume would be larger. Therefore, our hypothesis was that regional SVg variations are able to identify target areas for LVRS, to quantify their extension, and to assess their connection with other regions. To verify these hypotheses, we analyzed SVg in the entire lung, in the different lobes, and in selected regions of interest belonging to all bronchopulmonary segments in healthy volunteers and patients with COPD in whom CT images were taken at high and low lung volumes.

Materials and Methods

Subjects

CT imaging was performed on 10 healthy volunteers with no history of smoking or lung disease and 10 patients with severe COPD belonging to a pretreatment assessment database of a clinical trial.¹⁴ The institutional review board of Washington University approved the protocol for healthy humans (HRPO n. 09-0602), and informed written consent was obtained from each subject. Local institutional review board approval was obtained, and written informed consent was obtained from all patients with COPD.

CT Imaging

All subjects underwent scanning with a multidetector CT scanner (SOMATOM Sensation; Siemens AG). After coaching, CT scan was performed during a breath-hold in both deep inspiration (approximating total lung capacity [TLC]) and deep expiration (approximating residual volume [RV]) with the subject in the supine position. The subjects were instructed on the importance of breath-holding and immobility during scanning and on attaining reproducible maximum inspiratory and expiratory breath-hold.

The voxel size was $0.625 \times 0.625 \times 1$ mm, x-ray tube current 160 mA, kVp 120, pitch 1, and effective mAs 160 in CT images of healthy subjects. CT images of patients with COPD had a variable slice thickness (0.6-2 mm). All the CT images were reconstructed with a standard reconstruction filter (b50f). The resulting radiation dose was approx-

imately 2.4 and 2.5 to 2.7 mSv per scan, respectively, in healthy subjects and patients.

Image Analysis

Lung/Lobes Segmentation and Volume Calculation: CT images of the lung were first segmented by means of an automatic algorithm based on the method proposed by Hu et al.¹⁵ Left and right lungs were separated by detecting the anterior and posterior junctions, and lung boundaries along the mediastinum were smoothed. The lobes were segmented using MIPAV software (National Institutes of Health, <http://mipav.cit.nih.gov/>). As in some cases the fissure was not clearly visible, right middle lobe was grouped with the right upper lobe (RUL). The voxels with intensity below -600 HU were considered to be parenchymal, and the volume of the whole lung (tissue and airspace) was computed as the sum of the volumes of the voxels in each segmented slice, calculated as the product of the pixel size and the reconstruction interval spacing between slices.⁵

Region of Interest Selection: A three-dimensional airway reconstruction was used to choose a region of interest (ROI) in each lung segment (see later) at the two different lung volumes (Fig 1). An automatic algorithm using a region-growing approach, based on the iterative algorithm proposed by Kiraly et al,¹⁶ was developed to segment airway trees. The airways segmentation began by selecting a seed point in the trachea. The regions to be segmented were identified by means of voxel connectivity and inclusion criteria. Considering the seed point as the first point of the segmented region, the HU

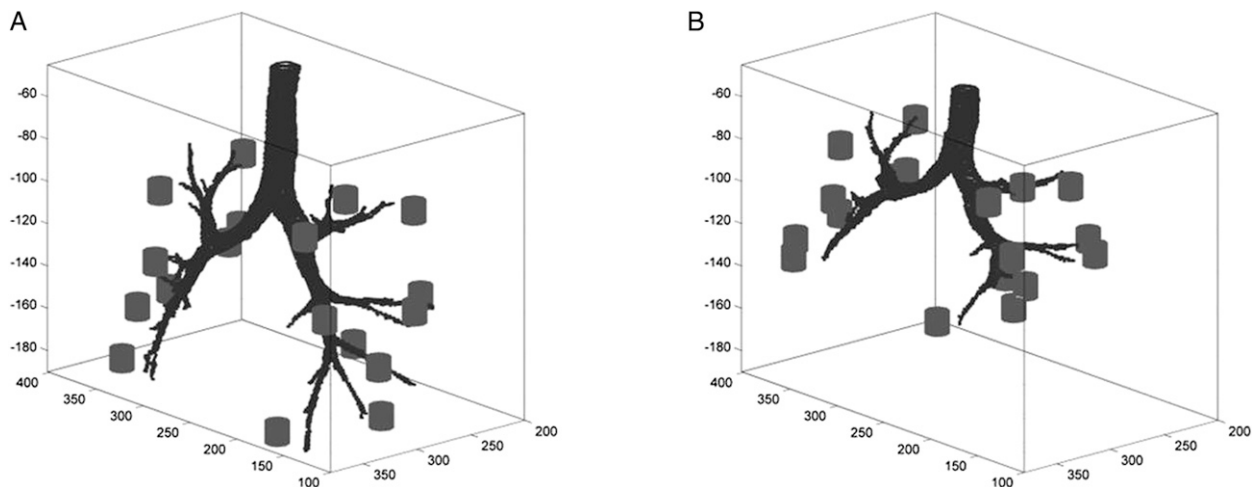


Figure 1 – Example of a three-dimensional airway reconstruction used to define the cylindrical region of interest in all the bronchopulmonary segments at the two different lung volumes. A, TLC. B, RV. RV = residual volume; TLC = total lung capacity.

intensity of each voxel belonging to a 26-member neighborhood of the seed point was checked and added to the segmented region if it was below a certain threshold.¹⁷ The optimal intensity threshold was the maximum intensity threshold that did not result in parenchymal leakage (ie, the condition where the segmented region “leaks” out of the airways and includes a large number of voxels belonging to the parenchyma). The segmentation was completed by a morphologic closing and hole-filling step. The airway trees were reconstructed to the level of subsegmental bronchi, or later subdivisions in some cases.¹⁷ The selected ROI in each segment was a cylinder constructed by choosing a circle on a selected slice, clearly within the bronchopulmonary segment of interest, with a diameter of 10 mm and extending 5 mm below and above this central slice. The circle was chosen distal to a segmental bronchus but not overlapping it and clearly avoiding the inclusion of voxels belonging to any airway.

Quantitative Analysis: All quantitative analysis was performed by a custom software developed in Matlab (The MathWorks, Inc).⁷ Parenchymal analysis was performed for the entire lung, the different lobes, and all bronchopulmonary segments, in terms of SVg, defined as the difference between specific volume of tissue and gas and the specific volume of tissue and expressed as milliliters (gas)/grams (tissue).⁶ Specific volume of tissue and gas is the inverse of density as measured from CT scan, which is calculated by adding 1,024 to the HU of each voxel and then dividing by 1,024.⁶ The value used for the specific volume of tissue is the inverse of mean tissue density and calculated as specific volume of tissue = 1/1.06 mL/g.¹⁸ For the calculation of SVg, voxels belonging to airways, blood vessels, and other structures of the lung were excluded, and only those belonging to the parenchyma (ie, with HU values < -600 HU) were considered. Changes of SVg ($\Delta SVg = SVg_{TLC} - SVg_{RV}$, expressed as mL/g, where SVg_{TLC} and SVg_{RV} are specific gas volume at TLC and RV, respectively) relative to the corresponding whole-lung volume variations ($\Delta V = V_{TLC} - V_{RV}$, expressed as mL, where V_{TLC} and V_{RV} are lung volume at TLC and RV, respectively) were calculated as $\Delta SVg/\Delta V$ and expressed per milligrams.

According to a recently published study,¹⁹ the percentage of the voxels with attenuation values ≤ -950 HU (in CT images taken at TLC [LAA-950]) and ≤ -856 HU (in images taken at RV [LAA-856]) was calculated to estimate the extent of emphysema and gas trapping. To obtain global and lobar estimates, percentages were calculated respectively for the entire lung (LAA-950,total and LAA-856,total) and the different

lobes (LAA-950, lobar and LAA-856, lobar), namely RUL, right lower lobe (RLL), left upper lobe (LUL), and left lower lobe (LLL).

For each subject, a plot including all the segments connecting the values of SVg (expressed as percentage of SVg_{TLC}) and of lung volume (expressed as percentage of predicted TLC volume) at TLC and RV for each bronchopulmonary segment was constructed (gray lines in Fig 2). In the same plot, the segment relative to the overall lung was included (black line in Fig 2). A heterogeneity index (HI) was then defined for each subject as

$$HI = \frac{\sqrt{\left(\sum_{i=1}^N d_i^2\right)/N}}{\Delta V}$$

where N is the total number of the considered bronchopulmonary segments; d_i is the vertical distance (in the diagram) between the end point of the i^{th} bronchopulmonary segment and the end point of the overall lung at RV; and ΔV is lung volume change.

Sensitivity Analysis on $\Delta SVg/\Delta V$: To evaluate the effects of the arbitrary selection of the ROI within a given bronchopulmonary segment on $\Delta SVg/\Delta V$, in three patients with COPD (P1, P2, and P3), nine different ROIs were considered for each bronchopulmonary segment, by varying ROI size (three sizes, diameter from 10-20 mm and height from 6-22 mm) and ROI position (three positions within the same segment). For each segment, the deviation from the average $\Delta SVg/\Delta V$ was calculated. The range of variability in $\Delta SVg/\Delta V$, exclusively due to the arbitrary selection of the ROI within a given bronchopulmonary segment, was then defined as the 25th to 75th percentile range of the overall distribution of the 432 (nine ROIs, 16 bronchopulmonary segments, three subjects) values obtained as described.

Statistical Analysis

To compare SVg data, a three-way analysis of variance was performed with volume (RV and TLC), lobe (upper and lower), and disease (healthy and COPD) as independent factors. To compare $\Delta SVg/\Delta V$ data, a two-way analysis of variance was performed with lobe and disease as independent factors. Post hoc tests were based on the Holm-Sidak method. Linear regression analysis was applied to analyze possible relationships between % low attenuation area (LAA) and SVg and ΔSVg . Significance was determined by P values $< .05$.

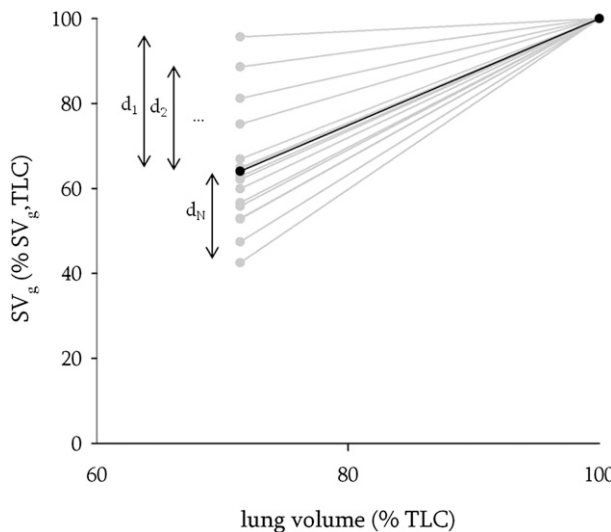


Figure 2 – Representative plot including all the segments connecting the values of SV_g (expressed as percentage of SV_g at TLC, SV_g, TLC) and of lung volume (expressed as percentage of predicted TLC volume) at TLC and RV for each bronchopulmonary segment (gray lines) and the segment relative to the overall lung (black line). d = distance between the end points of each bronchopulmonary segment and the end point of the overall lung at RV. N = total number of the considered bronchopulmonary segments. SV_g = specific gas volume. See Figure 1 legend for expansion of other abbreviations.

Results

Anthropometric characteristics, spirometric parameters, total LAAs, and lung volume (calculated from CT images) are reported in Table 1 for both patients with COPD and healthy subjects. Individual values of LAA-950 and LAA-856 in the different lobes are shown in Table 2. Individual total and lobar values of mean values of SV_g at RV and TLC are shown in Table 3. The group of healthy subjects (aged 41-62 years) had normal spirometry for their ages, FEV_1/FVC values 70%, and $RV/TLC < 32\%$. Patients were characterized by values of total and lobar %LAA-950, %LAA-856, lung volumes, and RV/TLC ratio ($> 65\%$) indicating severe and very severe emphysema, gas trapping, and a high degree of lung hyperinflation.¹⁹ Absolute SV_g values in patients with COPD were dramatically higher than healthy control subjects, in the whole lung and in all lobes, both at RV and TLC.

Figure 3 reports average values of SV_g at TLC and RV in patients with COPD and healthy subjects for all the considered bronchopulmonary segments. In patients, the segments belonging to the right middle lobe (RB4 and RB5) were not included in the analysis because of the difficulty in obtaining reliable segmentation in these regions. The average and intersubject variability (ie, SD) of SV_g in the different bronchopulmonary segments, both at TLC and RV, was much higher in subjects with

COPD than in healthy subjects ($P < .001$). SV_g values at TLC were significantly different than SV_g values at RV in healthy subjects ($P < .001$) but not in subjects with COPD ($P = .067$).

In healthy subjects, SV_g values in the upper lobes were not significantly different than those in the lower lobes ($P = .55$), whereas in COPD, SV_g was significantly greater in the upper compared with the lower lobes ($P = .02$) (Table 3). The relationships between ΔSV_g and lung volume variation were very similar in all healthy subjects. Conversely, a great intersubject variability was found in COPD.

Figure 4 illustrates two examples, a patient with COPD and a representative healthy subject. In the patient, a high variance of the slopes (both positive and negative) of the straight lines connecting SV_g and volume values at TLC and RV was found. On the contrary, in the healthy subjects the slopes were very similar for the whole lung (black solid line), all lobes (black dashed lines), and bronchopulmonary segments (gray lines).

Figure 5 demonstrates that these findings can be generalized. In the same panel, the straight lines connecting SV_g and volume values at TLC and RV, for the whole lung and the different lobes, averaged in all healthy control subjects and all patients with COPD, are shown. Although in the control subjects all straight lines were very similar ($P = .741$), in the patients with COPD the straight lines of the different lobes were more largely distributed around the line of the entire lung, with upper lobes being above (lower slope) and lower lobes below (greater slope) ($P < .001$). Interestingly, the slopes in the upper lobes were significantly greater in control subjects than in subjects with COPD ($P < .001$), whereas in the lower lobes the slopes were similar between healthy subjects and subjects with COPD ($P = .956$).

Figure 6 reports the values of $\Delta SV_g/\Delta V$ ("slopes") of all bronchopulmonary segments in all subjects. Although overall average values of slopes were very similar between healthy subjects and those with COPD (2.76/mg and 2.82/mg, respectively), overall variability was significantly higher in patients with COPD ($SD = 3.80/mg$, $P < .001$) and very low in the healthy ($SD = 0.81/mg$). In Figure 6A, the upper limit of significant negative values of slopes, calculated as the 25th percentile in the distribution of slopes exclusively due to ROI selection ($-1.79/mg$, dashed vertical line), is shown. Six out of 10 patients had bronchopulmonary segments with significantly negative slopes. Intrasubject

TABLE 1 Anthropometric Characteristics, Spirometric Parameters, Total Percentage of LAA-950 and LAA-856, and Lung Volume (Calculated From CT Images) for Patients With COPD and Healthy Subjects

Subjects	Sex	Age, y	Weight, kg	Height, cm	FEV ₁ , % Pred	FVC, % Pred	FEV ₁ /FVC, % Abs	% LAA-950	% LAA-856	V _T TLC, mL	V _{RV} , mL
COPD											
P1	F	65	68	163	28	63	35	32	71	6,049	4,387
P2	F	55	50	163	16	38	33	37	81	4,624	3,891
P3	F	54	57	170	n/a	n/a	23	35	66	6,356	5,732
P4	M	65	46	168	19	47	32	60	85	6,997	5,489
P5	F	67	49	170	18	55	24	38	81	5,891	5,240
P6	F	62	59	165	20	42	37	34	69	5,858	4,879
P7	M	71	80	178	16	63	19	57	83	9,327	6,459
P8	M	65	69	180	15	47	11	45	80	8,979	6,518
P9	F	54	64	165	17	50	27	35	47	5,902	4,214
P10	F	n/a	n/a	n/a	18	74	20	43	50	4,668	3,722
Mean	...	62	60	169	18	52	26	42	71	6,465	5,053
SD	...	6	11	6	4	11	8	10	13	1,585	1,006
Control											
S1	F	54	76	173	135	140	78	24	19	6,028	1,873
S2	M	62	75	180	123	114	86	23	11	5,915	1,192
S3	M	46	78	178	97	102	78	13	12	4,360	1,762
S4	F	44	60	163	134	138	81	23	37	5,338	2,804
S5	M	49	114	201	93	108	70	27	21	9,383	2,777
S6	F	46	68	165	113	121	77	20	6	5,451	1,379
S7	F	41	81	155	91	96	80	14	1	3,728	949
S8	F	45	89	160	104	114	83	17	3	4,717	1,858
S9	F	42	89	173	108	127	71	24	4	5,560	1,356
S10	F	44	77	165	91	97	79	25	2	4,367	1,245
Mean	...	47	81	171	109	116	78	21	12	5,485	1,719
SD	...	6	15	13	17	16	5	5	11	1,560	640

abs = absolute; LAA-856 = lung pixels with an attenuation of ≤ -856 HU on expiratory CT scan; LAA-950 = lung pixels with an attenuation of ≤ -950 HU on inspiratory CT scan; n/a = data not available; pred = predicted; RV = residual volume; TLC = total lung capacity; V_TTLC = lung volume at residual volume; V_{RV} = lung volume at total lung capacity.

TABLE 2 Lobar Percentage LAA-950 and LAA-856 in Patients With COPD and in Healthy Subjects

Subjects	RUL		RLL		LUL		LLL	
	%LAA-950	%LAA-856	%LAA-950	%LAA-856	%LAA-950	%LAA-856	%LAA-950	%LAA-856
COPD								
P1	35	79	17	77	33	71	26	58
P2	66	89	60	85	60	86	65	85
P3	41	76	35	68	34	69	25	49
P4	54	79	45	63	54	81	67	89
P5	30	81	52	88	34	84	27	70
P6	29	66	33	68	18	48	48	82
P7	61	89	26	48	58	88	35	52
P8	52	91	26	72	53	93	11	57
P9	34	50	46	84	28	64	21	50
P10	42	73	46	78	44	77	25	50
Mean	44	77	39	73	42	76	35	64
SD	13	12	13	12	14	13	19	16
Control								
S1	29	30	16	24	26	24	14	9
S2	29	14	15	8	30	11	13	3
S3	15	17	9	16	17	13	11	16
S4	28	62	16	11	34	63	15	20
S5	32	33	28	5	34	27	28	4
S6	30	8	25	2	23	4	16	4
S7	15	9	13	1	11	6	11	1
S8	14	20	12	3	14	17	13	5
S9	25	13	18	4	23	7	17	2
S10	24	15	20	4	24	2	20	12
Mean	24	22	17	8	24	17	16	7
SD	7	16	6	7	8	18	5	6

LLL = left lower lobe; LUL = left upper lobe; RLL = right lower lobe; RUL = right upper lobe. See Table 1 legend for expansion of other abbreviations.

variability of $\Delta SVg/\Delta V$, expressed by the HI calculated in each subject, was significantly higher in COPD than in healthy subjects (respectively, 0.80 ± 0.34 and 0.15 ± 0.10 ; $P < .001$).

In Figure 7, the relationships between lobar and total LAAs and the corresponding absolute values of SVg and $\Delta SVg/\Delta V$ are shown both in subjects with COPD (filled symbols) and control subjects (open symbols). In Figures 7A-D, for each value of lobar LAA-950 and lobar LAA-856 (x-axis), the values of SVg and $\Delta SVg/\Delta V$ of the different bronchopulmonary segments belonging to a given lobe are indicated on y-axis. In Figures 7E and 7F, for each value of total LAA-950 and total LAA-856 (x-axis), the values of $\Delta SVg/\Delta V$ of all the bronchopulmonary segments belonging to a given subject are indicated on the y-axis.

Discussion

CT imaging has been recognized as an important method for assessment of COPD. One of the approaches allowed by this technique is the calculation of specific volume of gas, which converts CT scan density into the physiologic meaningful index of volume of gas per gram of tissue. SVg is expected to change as a function of lung volumes. In the present work we measured SVg changes as lung volume decreases from a high volume close to TLC to a lower volume close to RV. The analysis was conducted not only for the overall lung but also locally, by considering the different lobes and by selecting small regions of interest corresponding to the different bronchopulmonary segments, in the same way that we envision future analysis for interventional targeting. This is of physiologic relevance, because total

TABLE 3 | Lung Volumes and SVg Values in the Different Lobes in Patients With COPD and Healthy Subjects

Subjects	Whole Lung			RUL			RLL			LUL			LLL		
	SVg,TLC, mL/g	SVg,RV, mL/g	Δ SVg, mL/g	SVg,TLC, mL/g	SVg,RV, mL/g										
COPD															
P1	11.9	8.9	3.0	13.9	10.9	11.7	7.1	14.8	10.9	10.4	7.3	7.3			
P2	38.6	35.5	3.2	56.2	58.1	33.6	25.5	46.8	45.0	29.4	22.6	22.6			
P3	29.3	27.3	2.1	33.4	30.6	29.2	25.8	28.2	26.9	25.7	23.1	23.1			
P4	41.6	33.1	8.5	40.1	32.5	35.7	28.3	38.9	31.6	47.4	39.4	39.4			
P5	14.4	13.4	1.1	12.2	12.1	14.3	12.1	12.2	12.0	18.5	15.6	15.6			
P6	17.3	14.1	3.2	11.8	9.5	24.7	21.1	10.0	6.9	21.9	18.2	18.2			
P7	45.4	40.1	5.3	57.5	52.4	23.0	19.0	52.0	47.6	30.5	22.4	22.4			
P8	20.5	17.2	3.3	24.1	21.6	17.7	11.3	25.1	23.0	13.0	10.5	10.5			
P9	16.0	10.2	5.7	17.1	11.0	18.2	12.0	14.7	9.4	14.3	8.5	8.5			
P10	37.5	34.7	2.8	35.7	33.1	43.7	42.7	36.8	34.0	34.3	29.6	29.6			
Mean	27.2	23.4	3.8	30.2	27.2	25.2	20.5	28.0	24.8	24.6	19.7	19.7			
SD	12.7	11.9	2.1	17.3	17.5	10.3	10.6	15.1	14.8	11.3	10.0	10.0			
Control															
S1	13.5	3.8	9.8	14.6	4.3	12.0	3.3	15.5	4.3	12.1	3.1	3.1			
S2	14.4	2.7	11.6	15.2	2.8	11.3	2.5	15.7	2.8	15.8	2.8	2.8			
S3	8.4	3.4	4.9	9.0	4.1	7.3	3.5	9.7	3.3	7.6	2.6	2.6			
S4	13.0	5.3	7.8	15.4	6.0	10.0	4.1	14.8	6.8	12.0	4.1	4.1			
S5	14.3	3.4	10.9	14.6	3.9	15.2	3.1	13.6	4.0	13.6	2.8	2.8			
S6	12.3	2.7	9.6	13.4	2.8	10.9	2.8	12.9	2.4	12.1	2.7	2.7			
S7	9.6	2.6	7.0	9.8	2.8	9.3	2.4	10.3	2.8	8.9	2.3	2.3			
S8	10.5	3.2	7.3	10.6	3.4	9.7	2.8	11.7	3.7	10.0	2.9	2.9			
S9	14.3	3.1	11.2	16.2	3.9	13.3	2.9	14.4	3.0	13.1	2.4	2.4			
S10	14.5	3.2	11.3	14.7	3.8	14.5	2.7	14.6	3.5	14.0	2.7	2.7			
Mean	12.5	3.3	9.1	13.3	3.8	11.4	3.0	13.3	3.7	11.9	2.8	2.8			
SD	2.2	0.8	2.3	2.6	1.0	2.4	0.5	2.1	1.3	2.5	0.5	0.5			

All data are obtained from CT images taken at TLC and RV. SVg = specific gas volume. See Table 1 and 2 legends for expansion of other abbreviations.

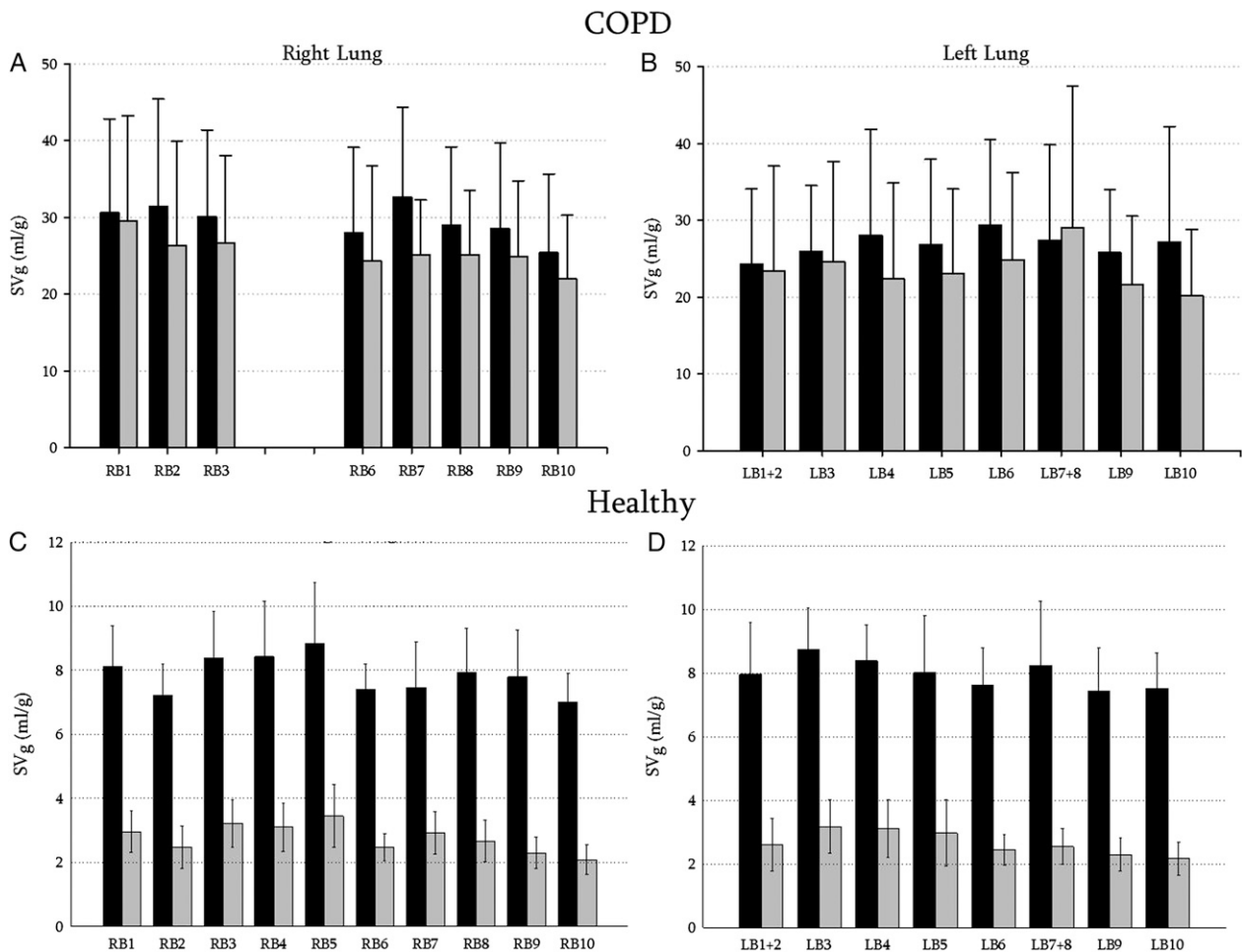


Figure 3 – A-D, Average values of SV_g at TLC (black bars) and RV (gray bars) in patients with COPD (A, B) and healthy subjects (C, D) for all the considered bronchopulmonary segments. Data are reported as mean \pm SD. See Figure 1 and 2 legends for expansion of abbreviations.

specific gas volume of the lung represents an average of all “regional” (ie, either lobes or bronchopulmonary segments) specific volumes ($SV_{g,r}$). If there are regions where $SV_{g,r}$ varies little with volume so that the slope of a plot of $\Delta SV_{g,r}$ against overall lung volume variation (ΔV) is smaller than that for both lungs, there must be other regions where $\Delta SV_{g,r}/\Delta V$ is steeper, indicating a greater than average decrease in $SV_{g,r}$ with decreasing volume. In normal lungs, there is no gas trapping above closing volume, so that the spread of values of $\Delta SV_{g,r}/\Delta V$ around their mean value is small (Fig 5). Conversely, in patients with COPD we found a considerably larger range of slopes, as shown in Figure 5, and quantified by the higher values of the HI, that allows quantifying in a single parameter the degree of heterogeneity in terms of regional lung emptying. Our results also indicate that the regions where $SV_{g,r}$ varies little with volume are mostly localized in the upper lobes, whereas lower lobes show similar $\Delta SV_{g,r}/\Delta V$ values.

Figure 6 illustrates that in emphysema the distribution of $\Delta SV_{g,r}/\Delta V$ slopes in the different bronchopulmonary segments is very wide compared with normal lungs, with more emphysematous lung regions having low values of $\Delta SV_{g,r}/\Delta V$ (left tail of the distribution plot in the figure), other regions remaining normal, and other regions having higher values (right tail of the plot). In other words, from this point of view in COPD the lung can be considered as a three-compartment system, in which one compartment groups all units with severe emphysema (regions with gas trapping and low values of $\Delta SV_{g,r}/\Delta V$), one groups all healthy units (regions with normal values of $\Delta SV_{g,r}/\Delta V$), and one groups all units with higher-than-normal values of $\Delta SV_{g,r}/\Delta V$. It is interesting to note that the occurrence of regions characterized by low values of $\Delta SV_{g,r}/\Delta V$ was similar in the different regions, with no significant differences between upper and lower lobes or between right and left lungs. As shown again in Figure 6 (left tail of the frequency distribution of $\Delta SV_{g,r}/\Delta V$), a significant

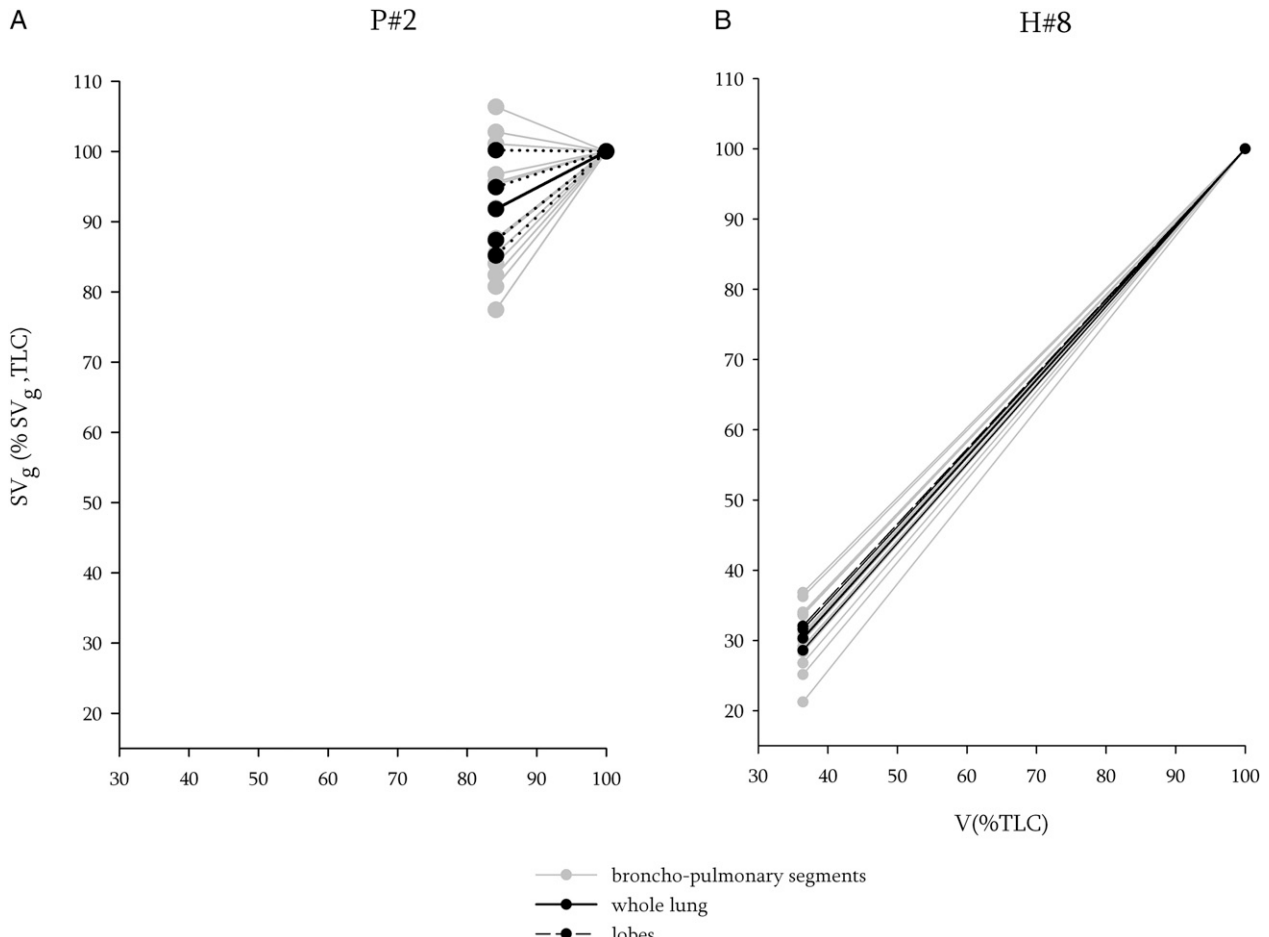


Figure 4 – A, B, SV_g expressed as % SV_g , TLC, as function of the lung volume (expressed as $V[\%TLC]$) in one patient with COPD (P#2) (A) and in a representative healthy subject (H#8) (B). Gray lines: segments connecting SV_g and volume values at TLC and RV in all bronchopulmonary segments. Dashed black lines: segments connecting SV_g and volume values at TLC and RV in the different lobes. Black lines: segments connecting SV_g and volume values at TLC and RV in the whole lung. $V[\%TLC] = \%TLC$ volume. See Figure 1 and 2 legends for expansion of other abbreviations.

number of bronchopulmonary segments in severe emphysema are characterized by significantly negative slopes in the $\Delta SVg, r / \Delta V$ plot (ie, SV_g increases when

lung volume decreases). This is also visible in the representative example reported in Figure 4, where the straight lines of three bronchopulmonary segments are

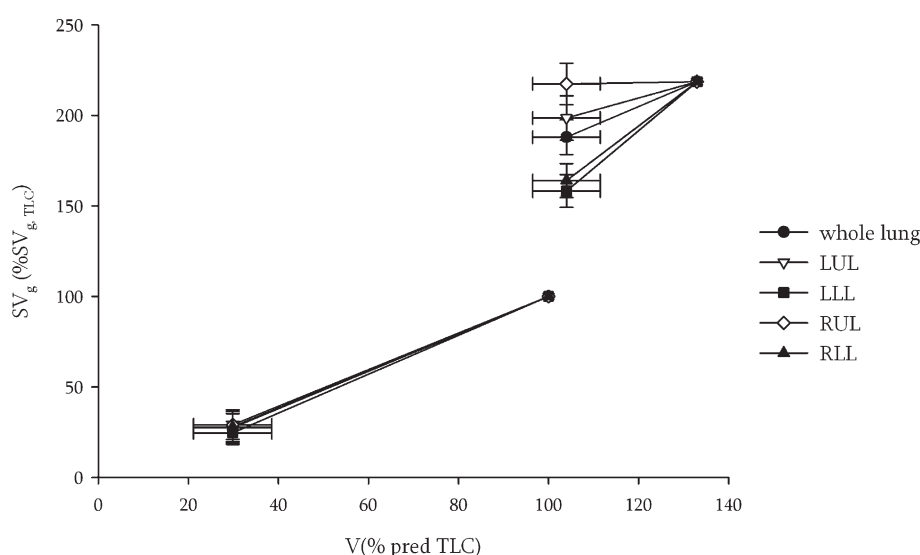


Figure 5 – SV_g expressed as % SV_g , TLC as function of the lung volume (expressed as pred %TLC volume). All segments connect SV_g and volume values at TLC and RV of the entire lung and all lobes. All points are reported as mean \pm SD of all patients with COPD and all healthy subjects. LLL = left lower lobe; LUL = left upper lobe; pred = predicted; RLL = right lower lobe; RUL = right upper lobe. See Figure 1 and 2 legends for expansion of other abbreviations.

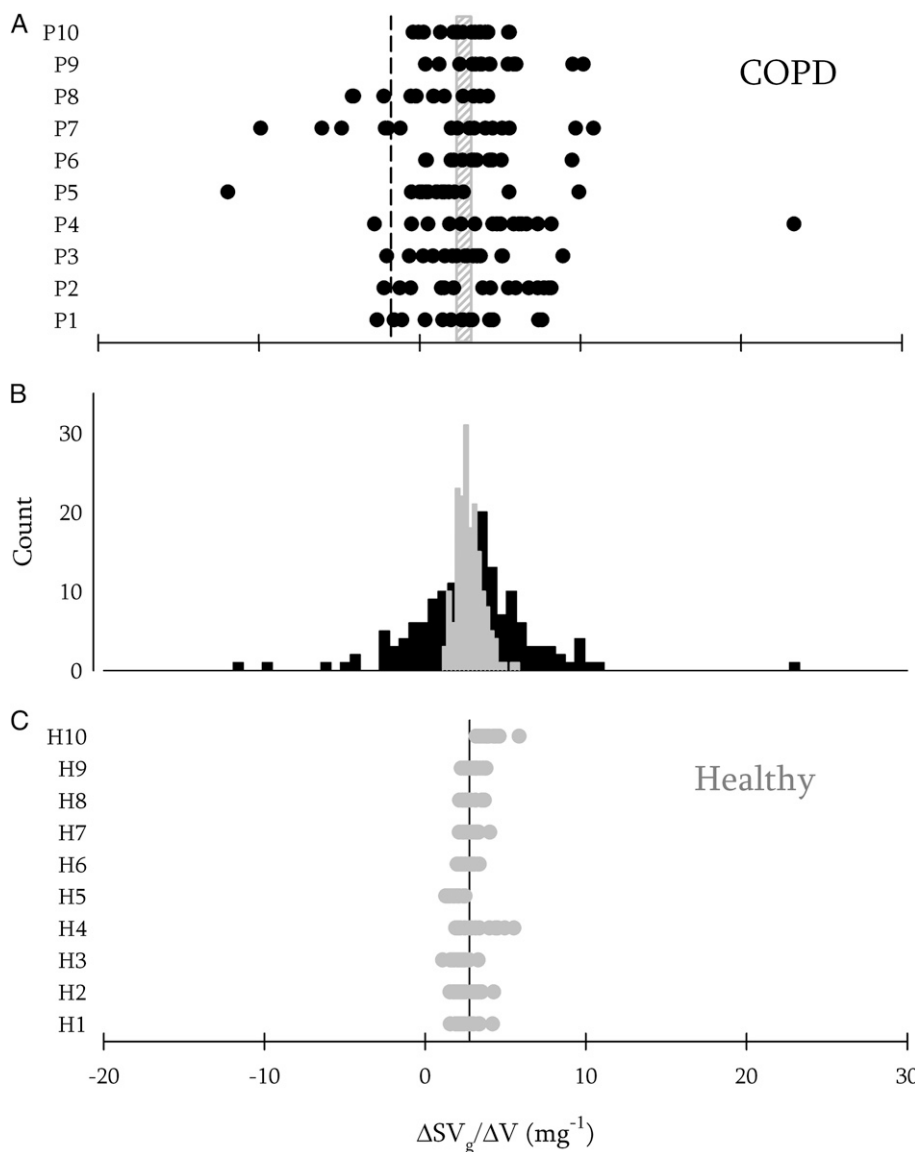


Figure 6 – A-C, Values of $\Delta SV_g/\Delta V$ of all bronchopulmonary segments in all individual patients with emphysema (A) and in all individual healthy subjects (C). B, Frequency distributions of all $\Delta SV_g/\Delta V$ values in all patients with emphysema (black) and all healthy subjects (gray). Vertical solid lines = means of all $\Delta SV_g/\Delta V$ values. Dashed line: upper limit of significant negative values of slopes (see text). Gray area: range (25th-75th percentiles) of $\Delta SV_g/\Delta V$ values in healthy subjects. $\Delta SV_g = SV_g, TLC - SV_g, RV$; $\Delta V = \text{total lung volume variations}$ ($\Delta V = V, TLC - V, RV$). See Figure 1 and 2 legends for expansion of other abbreviations.

characterized by a negative slope. As we pointed out,²⁰ a possible mechanism underlying this phenomenon is the presence of collateral flow through collateral channels in the emphysematous lung.²⁰ On the contrary, as the collateral ventilation is uniformly low in the healthy lung since the resistance to airflow is much greater through collateral channels than in the airway,^{20,21} all bronchopulmonary segments are characterized by positive slopes in the $\Delta SV_{g,r}/\Delta V$ plots. Figure 7F demonstrates that negative slopes are present in patients with $LAA-856 >$ approximately 60% (ie, the most severe in terms of total gas trapping)¹⁹ irrespective of the global extent of emphysema (Fig 7E). These findings are evident only when considering the relationships between $\Delta SV_{g,r}/\Delta V$ and total (not lobar) LAAs. Therefore, the main strength of $\Delta SV/\Delta V$ is to provide the chance

to study lung function locally, a possibility not provided by using LAAs calculated on smaller regions of the lung.

A limitation of the current study is represented by the dimensions of the regions of interest, which were of limited size compared with the segments, and by their positions within the segments, which were chosen to avoid possible intersections with the airways. The total number of subjects is relatively small, although results in the healthy group are quite narrowly distributed. All patients were characterized by severe COPD, which made them a somewhat homogeneous group.

The results of the regression analysis between $LAA-950$ and $SV_{g,TLC}$ (Fig 7A) and $LAA-856$ and $SV_{g,RV}$ (Fig 7B) indicate that although in healthy subjects absolute values of SV_g are obviously related to the amount of gas per

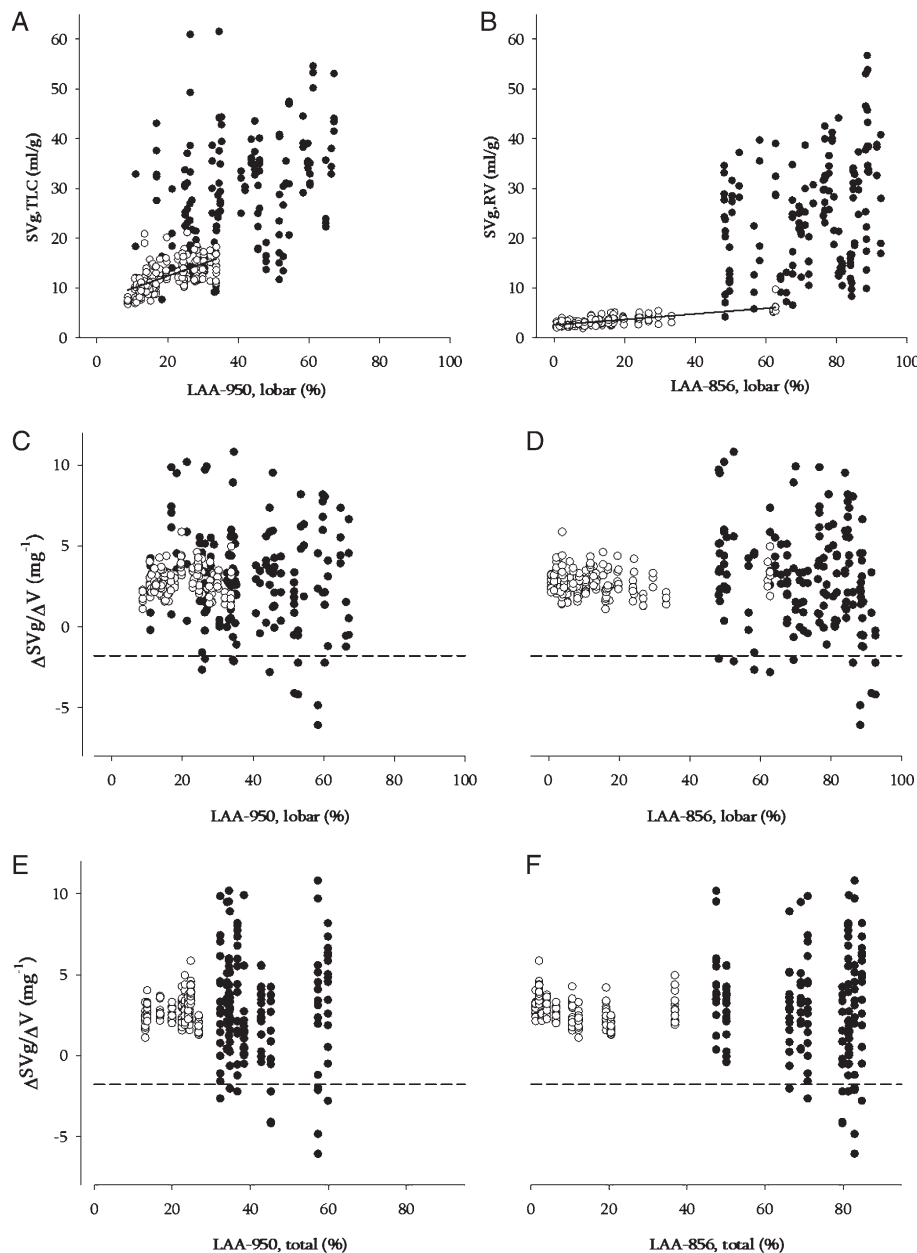


Figure 7 – Relationships between LAA, SV_g , and changes of SV_g relative to the corresponding whole lung volume variations ($\Delta SV_g/\Delta V$) in COPD (closed symbols) and healthy control subjects (open symbols). LAA expressed as percentage of voxels with density < -950 HU within a lobe at TLC (LAA-950, lobar), density < -950 HU within the entire lungs at TLC (LAA-950, total), density < -856 HU within a lobe at RV (LAA-856, lobar), density < -856 HU within the entire lungs at RV (LAA-856, total). A, B, C, D, For each value of either LAA-950, lobar (A and C) or LAA-856, lobar (B and D), the values of SV_g and $\Delta SV_g/\Delta V$ of the different bronchopulmonary segments belonging to a given lobe are indicated on y-axis. In E and F, for each value of total LAA-950, total and LAA-856, total (x-axis), the values of $\Delta SV_g/\Delta V$ of all bronchopulmonary segments belonging to a given subject are indicated on y-axis. Dashed horizontal straight lines (C-F): upper limit of significant negative values of slopes (see text). HU = Hounsfield unit; LAA = low attenuation area. See Figure 1 and 2 legends for expansion of other abbreviations.

lung tissue, in subjects with severe COPD they predict neither the extent of emphysema nor gas trapping. Only variations of SV_g are able to describe functional abnormalities. In fact, the identification of regions where $\Delta SV_g/\Delta V$ is low would help to identify and quantify regions (lobes and/or segments) where gas trapping is more pronounced. The identification of regions where $\Delta SV_g/\Delta V$ is negative, instead, would help to identify regions where collateral ventilation is present. The quantification of the heterogeneity index, finally, would be helpful to assess the patient in the different stages of disease and before/after different treatments.

To our knowledge, this is the first study that characterizes the healthy lung in terms of SV_g distribution measured from CT images of the lung at two different lung volumes. Therefore, the values here provided of SV_g (in the small range of 14–10.24 mL/g at TLC and 4.65–3.01 mL/g at RV) and $\Delta SV_g/\Delta V$ (in the small range of 2.76 ± 0.81 mg) obtained in the group of healthy subjects represent a reference for future studies in which SV_g and its changes with lung volume may be used as global and regional biomarkers for surgical planning and posttreatment evaluation of different techniques used for lung volume reduction in emphysema.

Acknowledgments

Author contributions: C. S., L. B., J. C. W., and A. A. had full access to the data, vouch for the accuracy and completeness of the data and the analyses, and were responsible for the decision to publish the manuscript. C. S., J. C. W., and A. A. contributed to conception and study design; J. C. W., contributed to data acquisition; L. B. and C. S. contributed to statistical analysis; and C. S., L. B., J. C. W., and A. A. contributed to data interpretation and drafting of the manuscript.

Financial/nonfinancial disclosures: The authors have reported to *CHEST* that no potential conflicts of interest exist with any companies/organizations whose products or services may be discussed in this article.

Role of sponsors: The sponsor had no role in the protocol design, analysis of data, or conception and writing of the manuscript.

Other contributions: This work is dedicated to Peter T. Macklem, MD, who inspired all the innovative ideas presented here.

References

1. Lutey BA, Lefrak SS, Woods JC, et al. Hyperpolarized 3He MR imaging: physiologic monitoring observations and safety considerations in 100 consecutive subjects. *Radiology*. 2008;248(2):655-661.
2. Woods JC, Choong CK, Yablonskiy DA, et al. Hyperpolarized 3He diffusion MRI and histology in pulmonary emphysema. *Magn Reson Med*. 2006;56(6):1293-1300.
3. Yablonskiy DA, Sukstanskii AL, Woods JC, et al. Quantification of lung microstructure with hyperpolarized 3He diffusion MRI. *J Appl Physiol* (1985). 2009;107(4):1258-1265.
4. Mata JF, Altes TA, Cai J, et al. Evaluation of emphysema severity and progression in a rabbit model: comparison of hyperpolarized 3He and 129Xe diffusion MRI with lung morphometry. *J Appl Physiol* (1985). 2007;102(3):1273-1280.
5. Coxson HO, Rogers RM, Whittall KP, et al. A quantification of the lung surface area in emphysema using computed tomography. *Am J Respir Crit Care Med*. 1999;159(3):851-856.
6. Coxson HO, Mayo JR, Behzad H, et al. Measurement of lung expansion with computed tomography and comparison with quantitative histology. *J Appl Physiol* (1985). 1995;79(5):1525-1530.
7. Salito C, Woods JC, Aliverti A. Influence of CT reconstruction settings on extremely low attenuation values for specific gas volume calculation in severe emphysema. *Acad Radiol*. 2011;18(10):1277-1284.
8. Salito C, Aliverti A, Gierada DS, et al. Quantification of trapped gas with CT and 3 He MR imaging in a porcine model of isolated airway obstruction. *Radiology*. 2009;253(2):380-389.
9. Shah PL, Slebos DJ, Cardoso PF, et al; EASE trial study group. Bronchoscopic lung-volume reduction with Exhale airway stents for emphysema (EASE trial): randomised, sham-controlled, multicentre trial. *Lancet*. 2011;378(9795):997-1005.
10. Venuta F, Rendina EA, Coloni GF. Endobronchial treatment of emphysema with one-way valves. *Thorac Surg Clin*. 2009;19(2):255-260.
11. Valipour A, Herth FJ, Burghuber OC, et al; VENT Study Group. Target lobe volume reduction and COPD outcome measures after endobronchial valve therapy. *Eur Respir J*. 2014;43(2):387-396.
12. Argula RG, Strange C, Ramakrishnan V, Goldin J. Baseline regional perfusion impacts exercise response to endobronchial valve therapy in advanced pulmonary emphysema. *Chest*. 2013;144(5):1578-1586.
13. Aliverti A, Pennati F, Salito C, Woods JC. Regional lung function and heterogeneity of specific gas volume in healthy and emphysematous subjects. *Eur Respir J*. 2013;41(5):1179-1188.
14. Broncus Technologies. EASE trial: exhale airway stents for emphysema. NCT00391612. ClinicalTrials.gov. <http://clinicaltrials.gov/ct2/show/NCT00391612>. Bethesda, MD: National Institutes of Health; 2006. Updated January 2011.
15. Hu S, Hoffman EA, Reinhardt JM. Automatic lung segmentation for accurate quantitation of volumetric X-ray CT images. *IEEE Trans Med Imaging*. 2001;20(6):490-498.
16. Kiraly AP, Higgins WE, McLennan G, Hoffman EA, Reinhardt JM. Three-dimensional human airway segmentation methods for clinical virtual bronchoscopy. *Acad Radiol*. 2002;9(10):1153-1168.
17. Salito C, Barazzetti L, Woods JC, Aliverti A. 3D airway tree reconstruction in healthy subjects and emphysema. *Lung*. 2011;189(4):287-293.
18. Rosenblum LJ, Mauceri RA, Wellenstein DE, et al. Density patterns in the normal lung as determined by computed tomography. *Radiology*. 1980;137(2):409-416.
19. Schroeder JD, McKenzie AS, Zach JA, et al. Relationships between airflow obstruction and quantitative CT measurements of emphysema, air trapping, and airways in subjects with and without chronic obstructive pulmonary disease. *AJR Am J Roentgenol*. 2013;201(3):W460-470.
20. Hogg JC, Macklem PT, Thurlbeck WM. The resistance of collateral channels in excised human lungs. *J Clin Invest*. 1969;48(3):421-431.
21. Macklem PT. Airway obstruction and collateral ventilation. *Physiol Rev*. 1971;51(2):368-436.